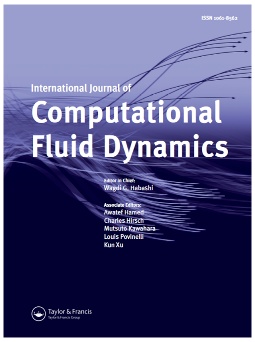

INTERNATIONAL JOURNAL OF COMPUTATIONAL FLUID DYNAMICS

ISSN: 1061-8562 (Print) 1029-0257 (Online) Journal homepage: www.tandfonline.com/journals/gcfd20

Computational Modelling of Non-Newtonian Effects on Flow in Channels with Moving Wall Indentations

X. QING & M. DAMODARAN

International Journal of Computational Fluid Dynamics, Vol. 15, pp. 329–336
Reprints available directly from the publisher
Photocopying permitted by license only

Short Communication

Computational Modelling of Non-Newtonian Effects on Flow in Channels with Moving Wall Indentations

X. QING and M. DAMODARAN*

Division of Thermal and Fluids Engineering, Centre for Advanced Numerical Engineering Simulations, Nanyang Technological University, Nanyang Avenue, Singapore, Singapore 639798

Non-Newtonian effects in a channel with moving wall indentations are assessed numerically by a finite volume method for solving the unsteady incompressible Navier–Stokes equations and using a power-law model exhibiting shear thinning viscosity and Casson's model as the constitutive equations for the non-Newtonian fluid. The computations show that for a non-Newtonian fluid, there are differences in the velocity profiles and in the structure and size of the reversed flow regions as compared with the corresponding Newtonian fluid. The comparison of non-Newtonian and Newtonian wall shear stress reveals a slight decrease in the magnitude on the average for the non-Newtonian case, eventually resulting in the strength of the "wave train" being slightly weaker than those corresponding to a Newtonian fluid.

Keywords: Physiological flow; Non-Newtonian flow; Moving boundary

1. INTRODUCTION

The study of blood flow in physiological systems such as arteries or the left ventricle of the heart is a complex flow problem involving moving boundaries, unsteady flow phenomena and non-Newtonian flow characteristics. The aim of this work is to examine the impact of non-Newtonian effects on the flow phenomena associated with moving boundaries, which will provide useful insight into further investigation of physiological fluid flows. In this study, Newtonian and non-Newtonian fluid flow in a channel with a moving wall indentation is investigated by modifying the mathematical flow model and the numerical solution method used by Demirdzic and Peric (1990) for modelling Newtonian flow for the same flow problem so as to assess the impact of non-Newtonian effects on the flow structure.

2. FLOW PROBLEM DEFINITION AND NUMERICAL MODELLING

The problem considered here is the unsteady Newtonian and non-Newtonian fluid flow through a channel with a wall indentation, which moves in a prescribed periodic manner. The geometric configuration of the flow domain is shown in Fig. 1 and the

*Corresponding author.

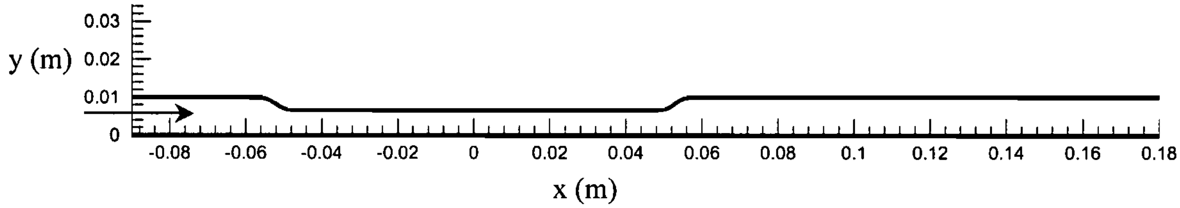

FIGURE 1 The geometry of the channel under investigation.

prescribed motion of the top wall is defined by Eq. (1)

$$y(x) = \begin{cases} 0.005\{1 - \cos(2\pi t^*)\} & \text{for } 0 < x < 0.04 \\ 0.005\{1 - \tanh[0.0414(x - 0.055)]\} & \text{for } 0.04 < x < 0.065 \\ 0 & \text{for } x > 0.065 \end{cases} \quad (1)$$

The mathematical model for this study is based on the unsteady incompressible Navier–Stokes equations for a Newtonian fluid and the finite volume numerical method for solving these equations follows closely the method outlined in Demirdzic and Peric (1990). Blood flow in the vicinity of moving boundaries is assumed to be non-Newtonian, homogeneous, unsteady and incompressible relative to the moving boundary. To simulate the non-Newtonian flow, an additional constitutive equation is required. As the motivation for the current investigation is to develop a method for the further simulation of physiological flows, two non-Newtonian blood models, i.e. the power-law model and the Casson model, are used to model non-Newtonian effects in the present calculation. According to Walburn and Schneck (1976) within the shear rate range of $0.031-120\,\mathrm{s}^{-1}$, the complex rheological properties of blood can be approximated using the power-law model [Eq. (2)] defined as

$$\mu = k\dot{\gamma}^{n-1} \quad (2)$$

where k is the consistency index, $\dot{\gamma}$ the shear rate and n the non-Newtonian index. For blood of 45% haematocrit at a temperature of 37°C, $k = 0.0134\,\mathrm{Pa.s}^n$ and $n = 0.785$ where the shear rate is expressed in s^{-1} and shear stress is expressed in $\mathrm{N/m}^2$. The Casson model is defined [Eqs. (3) and (4)] as in Whitemore (1968)

$$\sqrt{\tau} = \sqrt{\mu}\sqrt{\dot{\gamma}} + \sqrt{\tau_y}, \quad \tau > \tau_y \quad (3)$$

$$\dot{\gamma} = 0, \quad \tau < \tau_y \quad (4)$$

where τ_y is the yield stress taking a value of 0.0048 Pa and μ the dynamic viscosity such that $\mu = 0.0028\,\mathrm{Pa\,s}$. The two parameters characterising the present oscillatory flow are the Reynolds number ($Re = \rho bU/\mu$) and Strouhal number ($St = b/UT$), where U is the bulk velocity for flow through an uncollapsed channel of width of b. As comparison of non-Newtonian and Newtonian flows is the main focus of this work, the comparison is based on the Newtonian reference viscosity of $\mu_N = 0.0035\,\mathrm{N\,s/m}^2$. The density of the blood is taken to be $1050\,\mathrm{kg/m}^3$ for the numerical simulations.

Boundary conditions are specified at the inflow and outflow boundaries. At the inflow boundary, the flow in the channel upstream of the indentation is assumed to be a fully developed Poisseuille flow. At the outflow boundary, the components of the velocity gradients in the direction of the flow are set to zero. On the wall, the component of velocity along the direction parallel to the wall is set to zero while the component of velocity normal to the wall is set to the

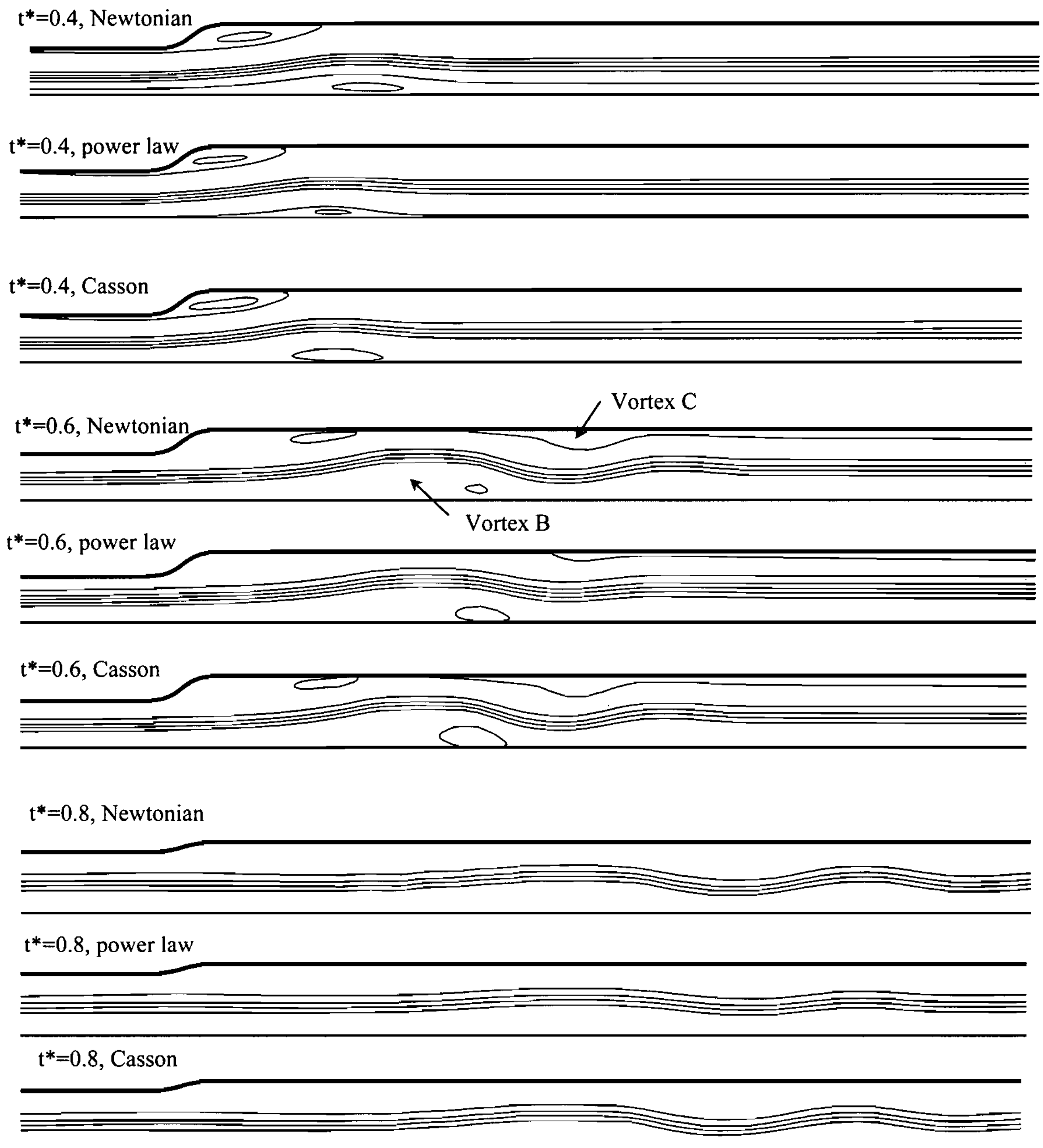

FIGURE 2 The comparison of computed streamline pattern variation with instantaneous time t^* for Newtonian fluid and power-law and Casson non-Newtonian fluids during one periodic cycle.

wall motion. The initial condition is set by assuming that the flow is fully developed everywhere so that unsteady computations can be initiated from this atet in a time-accurate manner.

3. RESULTS AND DISCUSSIONS

Grid dependence tests have been carried out for accuracy, and the results shown below are based on a

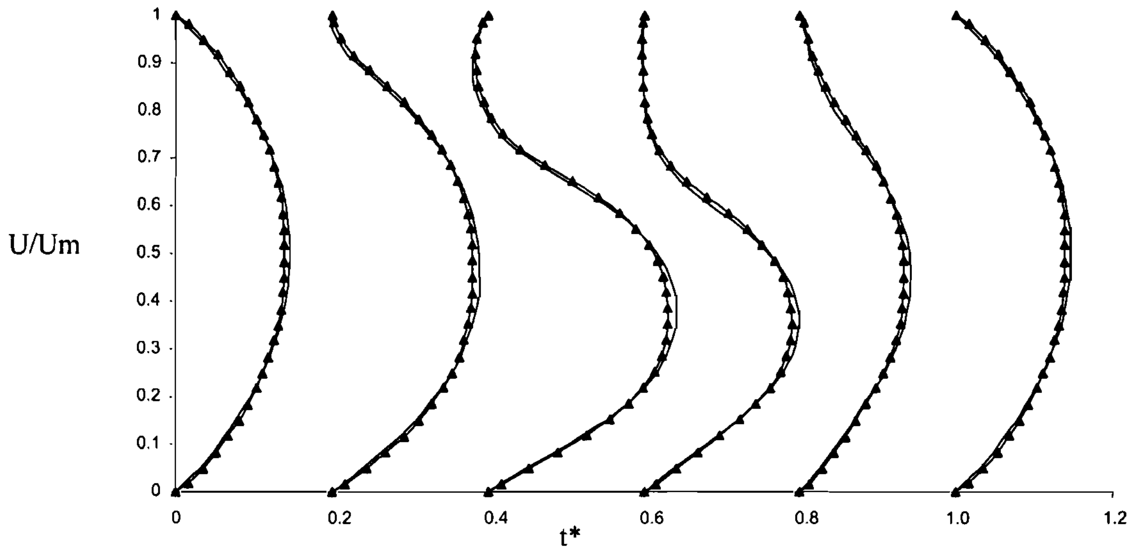

(a)

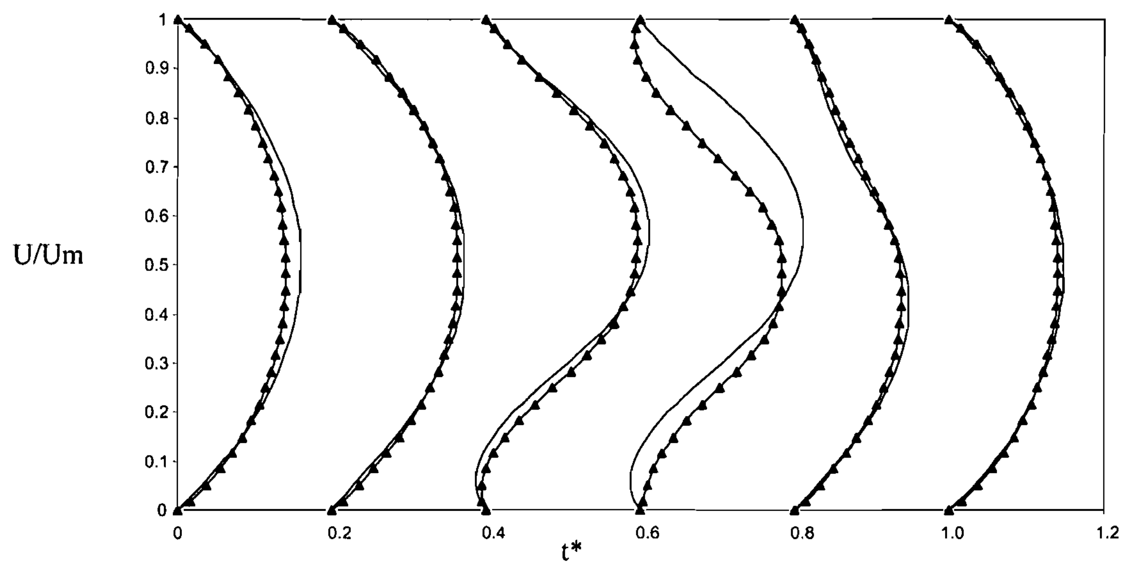

(b)

FIGURE 3 The development of the velocity profiles for Newtonian and power-law models during one cycle at locations: (a) $x/B = 5.25$; and (b) $x/B = 8.5$. (—) Newtonian fluid, (▲) power-law model.

fine computational mesh size consisting of 222×42 cells. The variation of the computed streamline patterns at different instants of time ($t^* = 0.4$, 0.6, 0.8) within one periodic cycle of the motion of the wall indentation for Newtonian, power-law and Casson fluids are compared in Fig. 2. The animation of the velocity field variation with the instantaneous time t^* for Newtonian and non-Newtonian power-law fluids during one cycle is shown in the attached movie file (*velocity.avi*). Note that the background colours

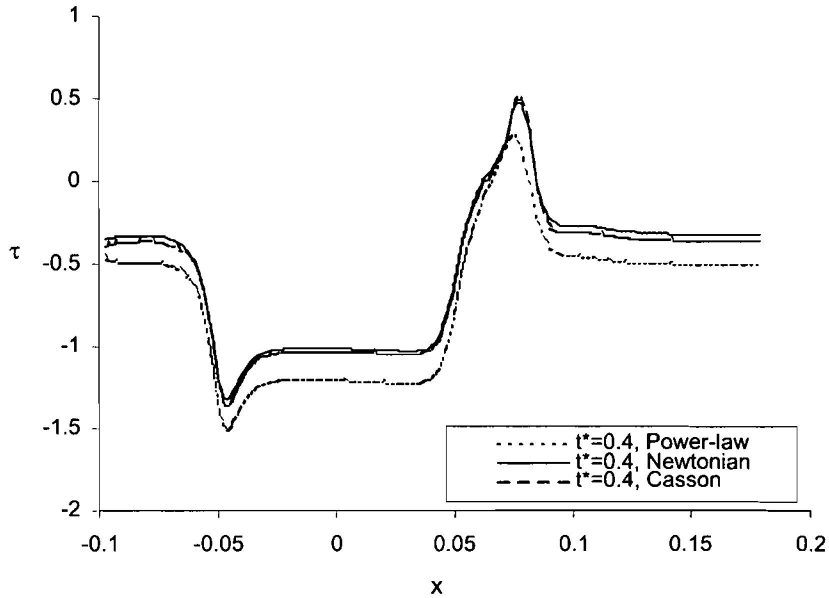
1
0.5
0
τ
-0.5
-1
-1.5
-2
t*=0.4, Power-law
t*=0.4, Newtonian
t*=0.4, Casson
-0.1
-0.05
0
0.05
0.1
0.15
0.2
x

(a)

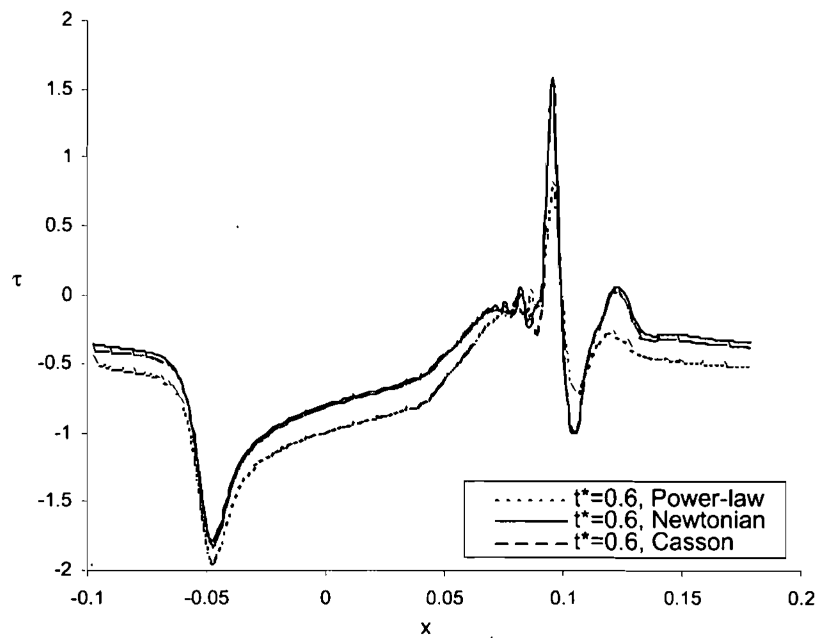
2
1.5
1
0.5
τ
0
-0.5
-1
-1.5
-2
t*=0.6, Power-law
t*=0.6, Newtonian
t*=0.6, Casson
-0.1
-0.05
0
0.05
0.1
0.15
0.2
x

(b)

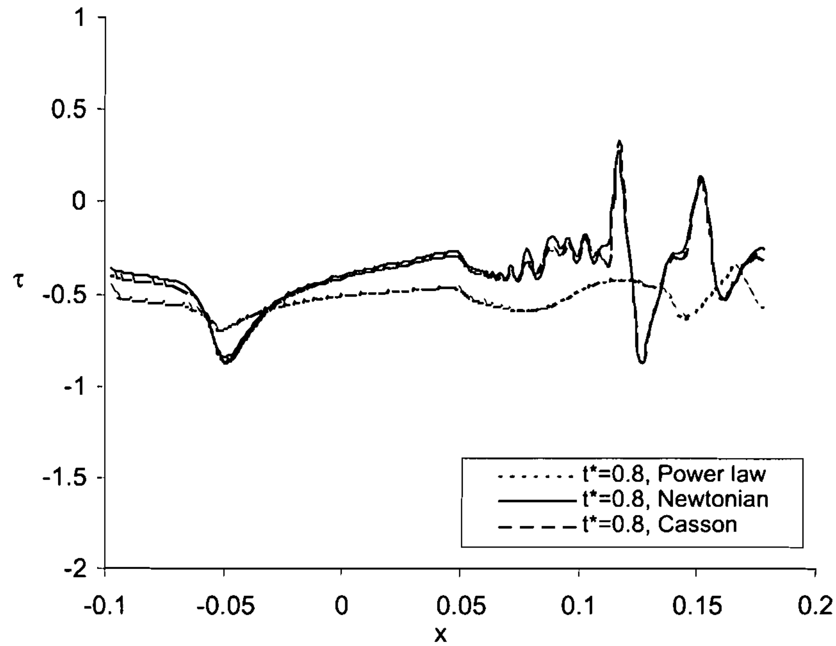

(c)

FIGURE 4 The comparison of Newtonian and non-Newtonain flows for wall shear stress distribution (on the indented wall) at different times: (a) $t^* = 0.4$; (b) $t^* = 0.6$; (c) $t^* = 0.8$.

in the movie correspond to the relative pressure contours. Comparison of these figures shows that the flow structure is generally not influenced by the non-Newtonian flow effects. However, a detailed comparison of the flow patterns clearly shows that the wave of vortices generated in the downstream of indentation differs slightly from each other. The velocity vector, computed using the Casson model, is closer to the corresponding Newtonian flow while they are different from the power-law flow. The strength of the vortices, which is reflected as the crests and troughs of the wave, seems weaker for the flow under the power-law model when compared with that of Newtonian and Casson flow. To clarify this aspect, Fig. 3(a) and (b) compares the velocity profiles for Newtonian and power-law models during one cycle at two specific locations downstream of the wall indentation at $x/B = 5.25$ and 8.5. In both figures, the horizontal axis corresponds to the value of the different instantaneous times t^*, while the vertical axis corresponds to the non-dimensional velocity U/U_m, and B is the localised channel width at $t = t^*$. It can be seen that for both Newtonian and non-Newtonian fluids, at a fixed location (x/B), the velocity profiles depart from the parabolic shape with the motion of the wall (i.e. as $t^* > 0$), and finally returns to it at the end of the cycle ($t^* = 1.0$). This phenomenon signifies the occurrence of the vortices during one cycle as a result of the upstream wall indentation. It can be seen that the reversed velocities signifying flow separation first occur at $t^* = 0.2$ and $x/B = 5.25$. Fig. 3(a) and (b) also shows that the major differences between Newtonian and non-Newtonian velocity profiles occur at $t^* = 0.6$, 0.8 when the top wall is moving back once the maximum amplitude is reached. This phenomenon implies that the non-Newtonian effects on the flow structure is more pronounced during the second half cycle, i.e. ($t^* > 0.5$).

Fig. 4(a)–(c) shows the variation of the computed wall shear stress on the wall indentation for Newtonian and two non-Newtonian flows at four

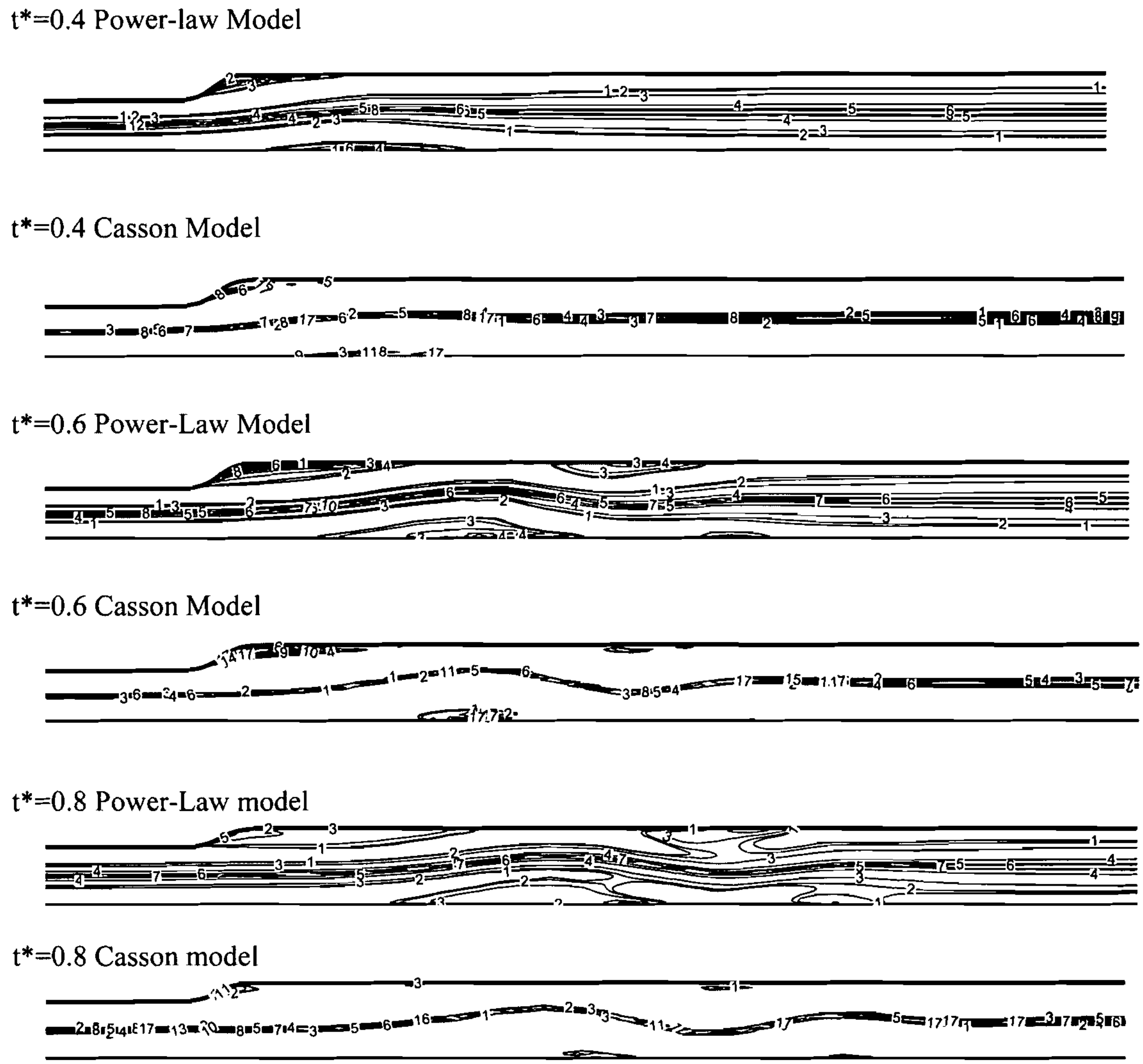

FIGURE 5 Computed contours of viscosity corresponding to Casson and power-law fluids (1:0.005466, 17:0.0321004, $d\mu = 0.0019067\,s^{-1}$).

specific instants of time, $t^* = 0.4$, 0.6 and 0.8. It can be seen that for all instances of t^*, the non-Newtonian shear stress distribution is similar to that of the Newtonian flow. However, at the same location (x) and same instant of time t^*, the shear stress corresponding to Newtonian and Casson flow generally has a higher value than those predicted by the power-law model. This can be seen clearly for $t^* \geq 0.6$.

Fig. 5 shows the computed contours of non-Newtonian viscosity at $t^* = 0.4$, 0.6 and 0.8. The differences in the contour lines can be clearly seen from the figures as t^* increases. As t^* increases during the cycle, the viscosity contours also exhibit a wave-like behaviour. Fig. 6 compares the computed positions of wave crests and troughs at different instants of time corresponding to their flow test case for which $St = 0.037$ and $Re = 507$ with the experimental measurements of Pedley and Stephanoff (1985). It can be seen that the computed results for both Newtonian and non-Newtonian fluids are in good agreement with these experimental measurements

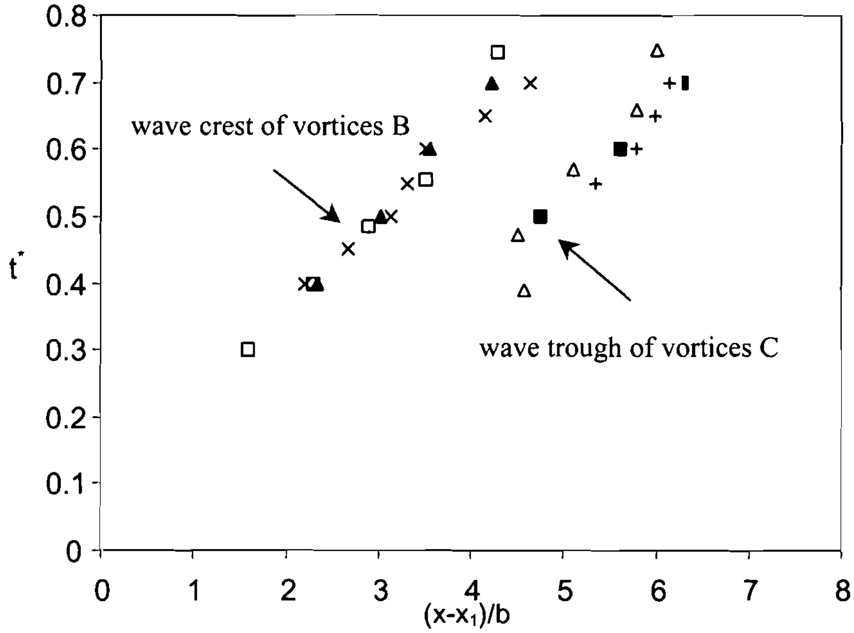

FIGURE 6 Comparison of the computed positions of wave crests of vortices B and wave troughs of vortices C corresponding to the flow for which $St = 0.037$, and $Re = 507$ with experimental results of Pedley and Stephanoff (1985). Legend for wave crests of vortices B: (□) experiments of Pedley and Stephanoff (1985); (×) computed power-law non-Newtonian flow; (▲) computed Newtonian flow. Legend for wave trough of vortices C: (Δ) experiments of Pedley and Stephanoff (1985); (+) computed power-law non-Newtonian flow; (■) computed Newtonian flow. Note that x_1 is the location at the middle of the downstream slope of the indentation.

even though minor quantitative differences can be seen. With regard to the non-Newtonian effect, the results of the power-law flow show a slightly lower value than the corresponding Newtonian flow.

4. CONCLUSIONS

In this work, unsteady incompressible Newtonian and non-Newtonian flows in a channel with a moving wall indentation have been computed. Rheological models for blood based on a simple power-law model exhibiting shear thinning viscosity and a Casson model displaying yield stress were used for the computation of unsteady non-Newtonian flows. On the basis of the computed velocity fields and wall shear stress distributions, it can be concluded that fluids obeying the Casson law behave basically as Newtonian fluids under the flow conditions investigated while fluids obeying the power law exhibit significantly different flow features than Newtonian fluids under the same flow conditions. Examination of the corresponding shear stress distribution and the maximum channel velocity enables the assessment of the impact of non-Newtonian effects for unsteady physiological flow fields that are considered in this study.

References

Demirdzic, I. and Peric, M. (1990) "Finite volume method for prediction of fluid flow in arbitrarily shaped domains with moving boundaries", *Int. J. Numer. Meth. Fluids* **10**, 771–790.

Pedley, T.J. and Stephanoff, K.D. (1985) "Flow along a channel with a time-dependent indentation in one wall: the generation of vortices waves", *J. Fluid Mech.* **160**, 337–367.

Walburn, F.J. and Schneck, D.J. (1976) "A constitution for whole human blood", *Biorheology* **13**, 201–210.

Whitemore, R.L. (1968) Rheology of the Circulation (Pergamon Press, Oxford).